Near-Infrared Resonance Raman Spectra of *Chloroflexus aurantiacus* Photosynthetic Reaction Centers†

Nerine J. Cherepy,‡ Alfred R. Holzwarth,§ and Richard A. Mathies*,‡

Department of Chemistry, University of California, Berkeley, California 94720, and Max-Planck-Institut für Strahlenchemie, Stiftstrasse 34-36, D-45470 Mülheim a.d. Ruhr, Germany

Received October 10, 1994; Revised Manuscript Received January 23, 1995⊗

ABSTRACT: Resonance Raman spectra of the photosynthetic reaction center isolated from the green bacterium *Chloroflexus aurantiacus* have been obtained with excitation in the near-infrared absorption bands of the special pair (P) and the accessory bacteriochlorophyll (B) using shifted-excitation Raman difference spectroscopy (SERDS). These spectra are compared with the previously reported Raman spectra of P and B in reaction centers from the purple bacterium *Rhodobacter sphaeroides.* The spectra of P and B from the two species are nearly identical. Common and distinctive attributes of these spectra include enhanced low-frequency (30−200 cm^{-1}) modes in P and the absence of strong Raman activity in modes higher than 1200 cm^{-1} in both P and B. Also, the absolute scattering cross sections with excitation in the P band are unusually weak in both reaction centers, indicating that their excited states are rapidly vibronically dephased. The striking similarities between the P and B spectra in reaction centers from two very different bacterial species suggest that the common nuclear and electronic dynamics identified here are characteristic of photosynthetic reaction centers.

Photosynthetic green bacteria are evolutionarily ancestral to the more widely studied purple bacteria (Woese, 1987). It is then reasonable that the photosynthetic reaction centers (RC)[1] of the purple bacterium *Rhodobacter sphaeroides* and the thermophilic green bacterium *Chloroflexus aurantiacus* show strong structural and functional similarities, starting with the utilization of bacteriochlorophyll *a* chromophores and extending to the kinetics of the charge separation processes. The RCs in these two species are highly homologous, but with several key differences that are summarized in the lower panel of Figure 1. The RC from *Rb. sphaeroides* contains 3 protein subunits called L, M, and H which serve as scaffolding for four bacteriochlorophyll (Bchl) molecules, two bacteriopheophytins (Bpheo), a non-heme iron atom, and two ubiquinones. The *C. aurantiacus* RC lacks the H subunit and contains three Bchls, three Bpheos, a manganese atom, and two menaquinones. The structure of the purple bacterial RC has an approximate C_2-axis of symmetry along which lie a special pair of bacteriochlorophyll *a*'s (P), two monomeric Bchls (B_A and B_B), and two Bpheos (H_A and H_B) (Allen et al., 1987; Deisenhofer et al., 1984). The A and B subscripts denote the active and inactive branches, respectively. Although a structure is not available, the chromophore arrangement for the *C. aurantiacus* RC is assumed to be the same as that for *Rb. sphaeroides*, except that the monomeric Bchl on the B branch is replaced by a bacteriopheophytin (Φ_B). The two RCs function very similarly with respect to electron transfer kinetics, quantum yield of charge separation, and electronic state structure of RC pigments (Becker et al., 1991; Boxer et al., 1989; Feher, 1989; Fleming & van Grondelle, 1994; Friesner & Won, 1989; Kirmaier et al., 1986; Müller et al., 1991; Pierson & Thornber, 1983; Volk et al., 1991). Following trapping of excitation into the lowest excited state, P*, charge separation between P* and H in *Rb. sphaeroides* occurs in about 3 ps at room temperature, while in *C. aurantiacus* charge separation occurs in 7 ps (Becker et al., 1991; Kirmaier et al., 1986; Müller et al., 1991; Shuvalov et al., 1986). In both RCs, electron transfer appears to proceed down only the A branch although some transient charge separation in the B branch has been proposed under certain conditions (Müller et al., 1991, 1992; Schweitzer et al., 1992).

The near-infrared absorption spectrum of the *C. aurantiacus* RC results from the Q_y electronic transitions of P, B, and H (see Figure 1). Three distinct peaks appear in this region, which in the room temperature spectrum are near 860, 810, and 760 nm. The 860-nm transition is due to P, the transition at 810 nm is mostly due to B, and the 760-nm transition is due to H and Φ_B. These same transitions occur in *Rb. sphaeroides* at 860, 800, and 760 nm. Thus, the *C. aurantiacus* RC differs in the Q_y absorption region by a reduced intensity and a slight red shift in the B band. The P band is essentially the same in both RCs; however, since the *C. aurantiacus* RC contains 3 Bpheos, the H band is more intense than in *Rb. sphaeroides*.

We are interested in developing a better characterization of the near-infrared electronic absorption bands of the two RCs and their underlying vibronic properties because this may help reveal the origin of differences in the kinetics and specify the functional properties of the chromophores

† This work was funded by a grant from the National Science Foundation to R.A.M. A.R.H. acknowledges the Max-Planck-Institut für Strahlenchemie for permission of leave of absence and for financial support during his stay in Berkeley.

* Address correspondence to this author.
‡ University of California.
§ Max-Planck-Institut für Strahlenchemie.

⊗ Abstract published in *Advance ACS Abstracts,* April 1, 1995.

[1] Abbreviations: P, special pair; B (B_A and B_B), accessory bacteriochlorophylls; SERDS, shifted excitation Raman difference spectroscopy; RC, reaction center; Bchl, bacteriochlorophyll; Bpheo, bacteriopheophytin.

0006-2960/95/0434-5288$09.00/0

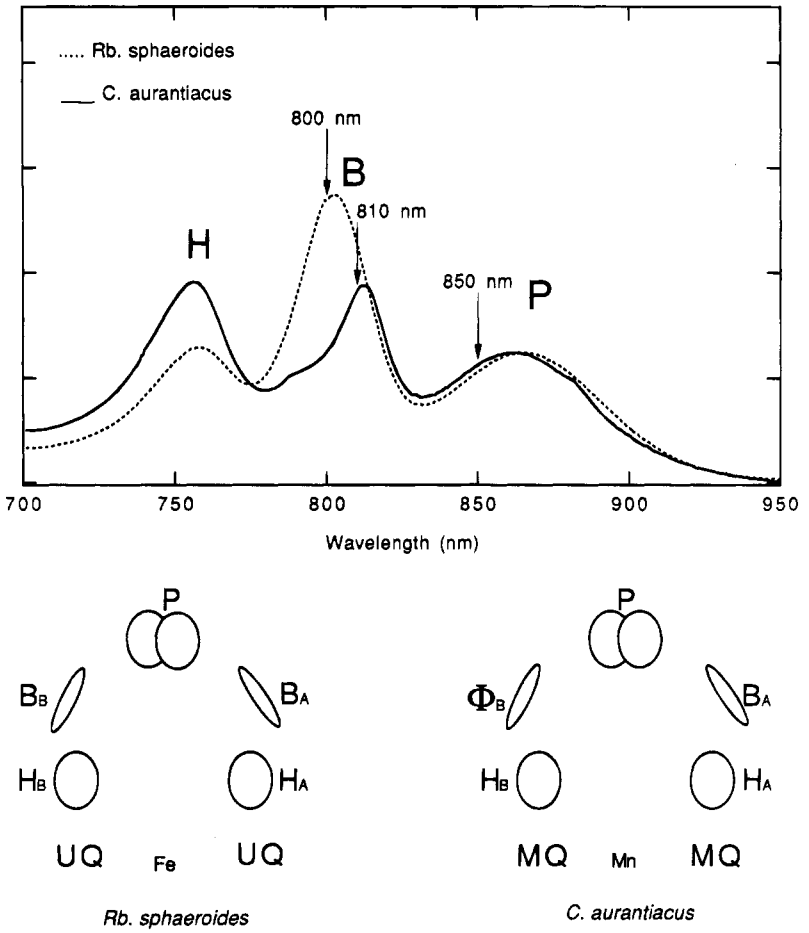

FIGURE 1: (Top) Near-IR absorption spectra of *C. aurantiacus* (—) and *Rb. sphaeroides* (- - -) RCs. Excitation wavelengths used for acquisition of resonance Raman spectra are indicated. The special pair, accessory bacteriochlorophyll, and bacteriopheophytin absorption bands are labeled P, B, and H, respectively. (Bottom) Schematic diagram of the chromophores in the RCs of *Rb. sphaeroides* and *C. aurantiacus*. Φ_B represents the bacteriopheophytin which is thought to occupy the position of B_B in the *C. aurantiacus* RC.

involved in this rapid and efficient photochemical electron transfer reaction. Raman spectra and resonance Raman intensities may be analyzed to give detailed information about nuclear distortions and electronic dynamics of the resonant transition; these parameters are particularly useful when studying photochemically-active transitions. Resonance Raman scattering intensities can also be used to determine the excited-state electronic dephasing time. For these reasons, we have developed methods for obtaining resonance Raman spectra with excitation in the lowest energy absorption bands of P and B and for determining the electron–nuclear coupling between the ground and excited states based on these data (Cherepy et al., 1994; Shreve et al., 1991, 1992). A characterization of the vibrational modes that couple the ground to the excited state will also be valuable in the interpretation of the excited-state stimulated emission oscillations seen in recent fs experiments on P (Vos et al., 1994). Here, we compare the resonance Raman spectra of RCs from *Rb. sphaeroides* and *C. aurantiacus* to examine the excited-state structure and dynamics of the chromophores involved in electron transfer. The similarities indicate which characteristics are common to the electron transfer mechanism, and the differences reveal how structure modification affects the system.

As in our previous work, shifted-excitation Raman difference spectroscopy (SERDS) is used to obtain Raman spectra of *C. aurantiacus* RCs in the presence of substantial background fluorescence (Cherepy et al., 1994; Shreve et al., 1991, 1992). Interestingly, we find that the patterns of normal modes observed for *Rb. sphaeroides* and *C. aurantiacus* RCs, are mostly conserved. In particular, the unique intense low-frequency modes observed in P from *Rb. sphaeroides* are also observed in *C. aurantiacus* RCs but these modes are not observed in the B spectra. In both the P and B spectra, only very weak scattering is observed in the high-frequency region (>1200 cm^{-1}), and the resonance Raman cross section for the characteristic 730 cm^{-1} mode is found to be an order of magnitude smaller with excitation in the special pair P than in B. The similarities and differences between the Raman spectra and scattering intensities in the two different RCs can be used to understand which aspects of the initial nuclear and electronic dynamics are common attributes of functioning bacterial reaction centers.

MATERIALS AND METHODS

RCs were isolated from *C. aurantiacus* as described in Müller et al. (1991) and suspended in buffer solution (0.025% lauryldimethylamine oxide, 10 mM Tris, 20 mM sodium ascorbate, pH 8) or in a 1/1 (v/v) mixture of buffer and ethylene glycol. Samples used to acquire the full spectra had an OD of 2–3 at the excitation wavelength in a 1 cm path length. Ethylene glycol-containing samples of OD ≈ 0.2/cm at the excitation wavelength (850 nm) were used to determine the absolute Raman scattering intensity of the 730 cm^{-1} mode.

Rapid-flow Raman experiments were performed using the same procedure we reported previously in studies of the R-26 carotenoidless mutant of *Rb. sphaeroides* (Cherepy et al., 1994; Shreve et al., 1991). The only change was the addition of a nitrogen gas purge in the flow cell reservoir to minimize oxidation of P. The sample flow velocity was about 200 cm/s, and the excitation power from a continuously-tunable Ti:sapphire laser ($\leq$5 mW at 850 nm) was cylindrically focused to an illumination area of about 5×10^{-4} cm^2. Assuming the extinction coefficient at 850 nm is identical in *Rb. sphaeroides* and *C. aurantiacus* RCs, these experimental conditions correspond to a photoalteration parameter of less than 0.3 (Cherepy et al., 1994). Emission spectra were recorded with a double spectrograph coupled to a liquid N_2-cooled CCD detector (LN/CCD-1152, Princeton Instruments). All reported spectra were corrected for wavelength dependence of the detection system by use of a standard lamp.

We used SERDS (Shreve et al., 1991, 1992) to identify RC Raman bands in the presence of the intrinsic fluorescence background from the P band ($\Phi_f > 4 \times 10^{-4}$) (Zankel et al., 1968). In this technique, two emission spectra are obtained with the excitation laser frequency shifted by 10 cm^{-1} relative to one another, but with all other experimental conditions identical. These spectra are then subtracted to yield a SERDS spectrum. In all reported spectra, the difference spectrum is the shifted minus the unshifted excitation spectrum, and the *x*-axis corresponds to the spectral axis for the unshifted excitation frequency. Derivative-like features, corresponding to Raman lines, are then fit to a model which assumes that the Raman spectrum is a difference of Gaussian peaks. The amplitude, position, and width of each peak is determined in a nonlinear least-squares fit, and these parameters are then used to generate the Gaussian peaks shown in the simulated Raman spectrum. Our previous work has demonstrated the accuracy of this method, by presenting directly-detected spectra (acquired with extended accumulation times) that match spectra simulated from the difference spectra (Shreve et al., 1991, 1992). The selection of spectral features to be fit was initially based on their reproducibility, shape (features with bandwidths of <2 and >15 cm^{-1} were not considered), and similarity to those previously observed for B and P. In analyzing the data presented here, we used a better band fitting program (Jandel PeakFit) than that employed in our previous work which allowed us to easily analyze more bands and to fit smaller features. In addition, the residuals of the fit were calculated to expose systematic differences, thereby providing a less subjective criterion for identifying additional bands. This procedure allowed us to fit and report here new bands in the *Rb. sphaeroides* P spectrum (the 622, 932, 1011, 1050, 1099, 1256, and 1278 cm^{-1} bands) and in the B spectrum (the 117, 397, 418, 436, 464, 478, 512, 920, 947, 970, and 1064 cm^{-1} bands). Some bands in the B spectrum were better fit with more than one mode (the feature at 731 cm^{-1} was fit with 3 modes at 721, 731, and 744 cm^{-1}, and the feature at 1010 was fit with two modes at 1001 and 1018 cm^{-1}). These features were all present in the raw SERDS data appearing in Figures 1 and 2 of Cherepy et al. (1994).

RESULTS

The resonance Raman spectra of *C. aurantiacus* RCs, exciting in the P and B absorption bands, are presented in Figures 2 and 3. The bottom two traces present the raw SERDS data and the residuals that result from the least-squares fit. The top traces present the simulated SERDS spectrum and the regenerated Gaussian spectra. For P, intense modes are seen from ~30 cm^{-1} out to 900 cm^{-1} with one particularly strong mode at 732 cm^{-1}. Some small features in the *C. aurantiacus* P spectrum were not fit, but are reproducible, such as those in the 350−550 cm^{-1} region. Spectra taken beyond 1000 cm^{-1} revealed no strong features. For B, scattering intensity is greatest from 200 to 1200 cm^{-1} with only weak modes beyond 1200 cm^{-1}. Due to limited quantities of sample, accumulation times for the *C. aurantiacus* spectra were shorter than for the *Rb. sphaeroides* spectra, thus reducing the overall signal-to-noise ratio. This is presumably why many smaller modes observed in the *Rb. sphaeroides* B spectrum are not seen clearly in the *C. aurantiacus* spectrum.

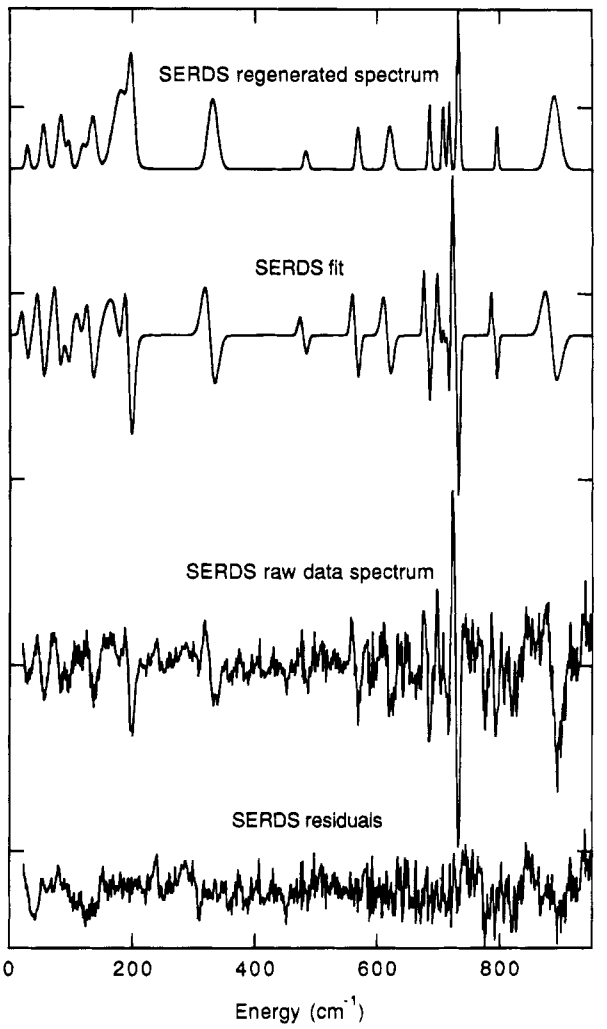

FIGURE 2: Shifted-excitation Raman difference spectra of P from *C. aurantiacus* RCs, obtained with 850-nm excitation and 5−6 cm^{-1} slits. The bottom two traces present the raw SERDS data and the residuals of the least-squares fit to these data. The top two traces present the simulated SERDS spectrum and the intensity-corrected, Gaussian-regenerated Raman spectrum of P.

The spectra of P and B share many Bchl modes in common, some of which have previously been assigned (Mattioli et al., 1990; Noguchi et al., 1991). For instance, the strongly coupled mode near 730 cm^{-1}, primarily a CNC in-plane deformation, has been observed in many spectral studies of Bchl and Bchl-containing species (Cherepy et al.,

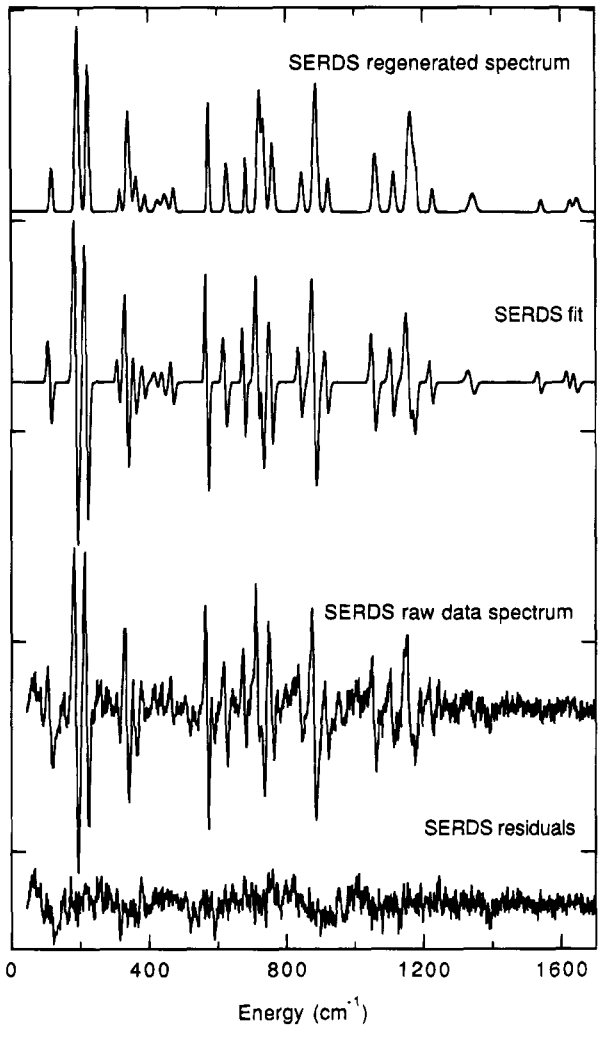

FIGURE 3: Shifted-excitation Raman difference spectra of B from *C. aurantiacus* RCs, obtained with 810-nm excitation and 5−7 cm^{-1} slits. The bottom two traces present the raw SERDS data and the residuals of the least-squares fit to the data. The top two traces present the simulated SERDS spectrum and the intensity-corrected, Gaussian-regenerated Raman spectrum of B.

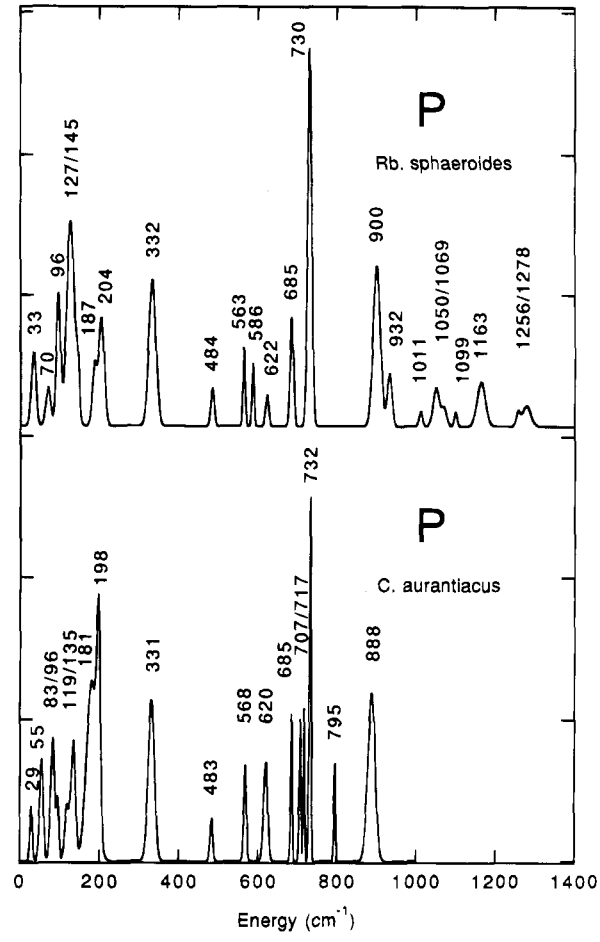

FIGURE 4: Comparison of the P resonance Raman spectra of *C. aurantiacus* and *Rb. sphaeroides*. The high-frequency region of the *C. aurantiacus* spectrum is not shown. Any features which appear above 1000 cm^{-1} are smaller than the noise in this region and much smaller than any of the features shown. The *Rb. sphaeroides* spectra have been adapted from Cherepy et al. (1994).

1994). We used this mode for quantification of resonance Raman scattering intensities. The absolute cross section of the 730 cm^{-1} mode with 850-nm excitation was measured by comparing its area with that of the 864 cm^{-1} mode of ethylene glycol as described by Cherepy et al. (1994). The average of four experiments gives about the same ratio of the 730 cm^{-1} cross section to the 864 cm^{-1} ethylene glycol cross section as that determined in the same experiment done on *Rb. sphaeroides* RCs, where this ratio was found to be $(2.2 \pm 0.6) \times 10^6$ (Cherepy et al., 1994). This is based on the assumption that the extinction coefficient of the *C. aurantiacus* RC at 850 nm is the same as that of *Rb. sphaeroides* (110 000 M^{-1} cm^{-1}).

DISCUSSION

The resonance Raman spectra of P and B from *C. aurantiacus* are compared with the corresponding spectra of P and B from the carotenoidless R-26 mutant of *Rb. sphaeroides* RCs in Figures 4 and 5. This comparison reveals that many mode frequencies and intensities are conserved in the spectra of both the P and B chromophores in *C. aurantiacus* and *Rb. sphaeroides* RCs. Where exact mode frequencies are not maintained, general intensity patterns are very similar. We will first discuss the spectra of P, followed by those of B, focusing on key similarities and differences.

The spectra of P from *C. aurantiacus* and *Rb. sphaeroides* are remarkably similar. In the low-frequency region, correlations between the two spectra for all the modes can be made. Since low-frequency modes are candidates for intradimer modes and displacement along such coordinates would possibly be involved in stabilizing excited-state charge transfer in P, it is of interest that this region does not differ much between species. The *C. aurantiacus* mode at 29 cm^{-1} matches the 33 cm^{-1} mode in the *Rb. sphaeroides* spectrum, and we correlate the 55 cm^{-1} *C. aurantiacus* mode with the *Rb. sphaeroides* 70 cm^{-1} mode. Similarly, the 83/95 cm^{-1} feature corresponds with the 96 cm^{-1} *Rb. sphaeroides* mode, the 135 cm^{-1} mode corresponds with the doublet at 127 and 145 cm^{-1} in *Rb. sphaeroides*, the doublet at 181 and 198 cm^{-1} corresponds to the *Rb. sphaeroides* doublet at 187 and 204 cm^{-1}, and the 331 and 332 cm^{-1} modes agree nearly exactly. Modes at 483 cm^{-1} appear in both spectra, while the *C. aurantiacus* mode at 568 cm^{-1} splits into the 563 and 586 cm^{-1} modes, and the 620 and 685 cm^{-1} modes match the 622 and 685 cm^{-1} *Rb. sphaeroides* modes. In the 700−800 cm^{-1} range, the *Rb. sphaeroides* spectrum contains only one mode at 730 cm^{-1}, while the *C. aurantiacus* spectrum

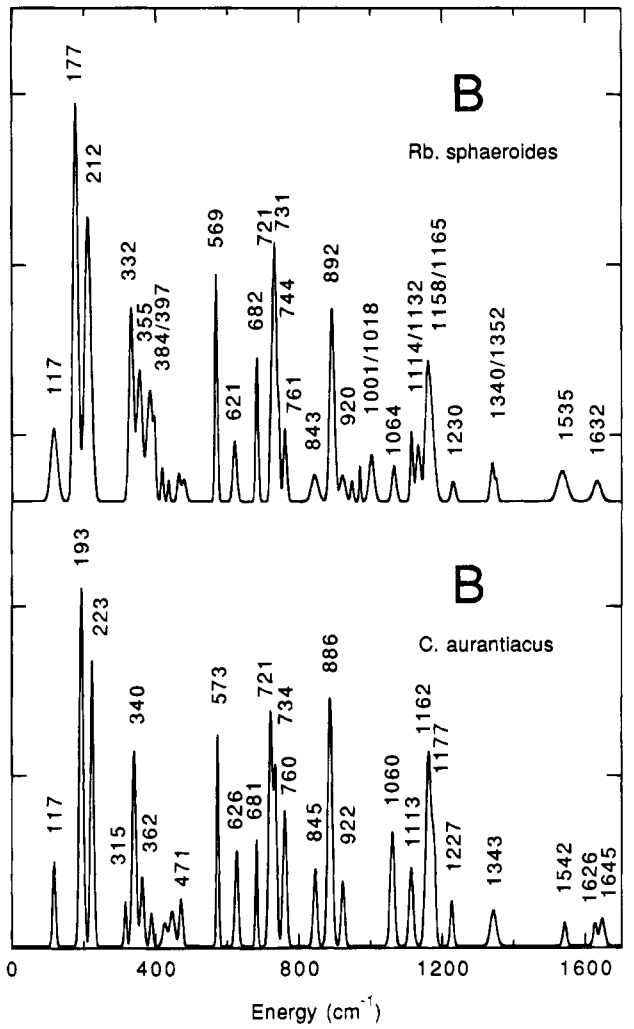

FIGURE 5: Comparison of the B resonance Raman spectra of *Rb. sphaeroides* and *C. aurantiacus*, obtained with 800 and 810 nm excitation, respectively. The *Rb. sphaeroides* spectra have been adapted from Cherepy et al. (1994).

has 4 modes at 707, 717, 732, and 795 cm^{-1}, all with small linewidths relative to the other bands in this spectrum. The narrow (~5 cm^{-1}) linewidths of the modes in the 700 cm^{-1} region, which were consistently observed in several independent data sets, are intriguing, particularly in comparison with the broad 888 cm^{-1} mode, which appears in the same data collection window. This variability of vibrational linewidths may be due to differences between the mode environments or arise from the presence of unresolved overlapping modes in the broader bands. Finally, the mode appearing at 888 cm^{-1} in *Rb. sphaeroides* is found at 900 cm^{-1} in *Rb. sphaeroides*. There are no strong modes in the high-frequency region of the *Rb. sphaeroides* spectrum, and survey spectra of this region in *C. aurantiacus* did not indicate any sizable modes beyond 950 cm^{-1}.

The two B spectra are also very similar. Focusing on the low-frequency region, it is notable that, compared to the P spectra, there is little activity, especially in the very low-frequency range (30−115 cm^{-1}) in either B spectrum. The 117 cm^{-1} mode is present in both species, the 193 and 223 cm^{-1} modes in *C. aurantiacus* shift to 177 and 212 cm^{-1} in *Rb. sphaeroides*, and a similar series of modes appear in both spectra in the 310−450 cm^{-1} range. There is a direct correlate for each of the *C. aurantiacus* B modes at 573, 626, 681, 721, 734, 760, and 845 cm^{-1} to modes in the *Rb. sphaeroides* spectrum. The remaining strong features in the B spectrum at 886, 1060, 1113, 1162, 1227, 1343, and 1542 cm^{-1} and the doublet at 1626/1645 cm^{-1} correspond to features in the *Rb. sphaeroides* spectrum, although there are a few weak modes in the *Rb. sphaeroides* spectrum whose counterparts were not observed or resolved in the *C. aurantiacus* spectrum. While little Raman activity is found in the high-frequency region of either B spectrum, they contain stronger modes beyond 950 cm^{-1} than the P spectra.

We have observed a remarkable similarity between the Raman spectra of P and B in *Rb. sphaeroides* and the spectra of P and B in *C. aurantiacus* RCs. However, the spectra of P and B presented here are not similar to those reported by Palaniappan et al. (1992, 1993). There are significant differences in mode frequencies, relative intensities, and absolute intensities. For example, while we found the absolute cross section of the 730 cm^{-1} mode with P resonance to be about 10 times smaller than the cross section with B resonance in the *Rb. sphaeroides* study (Cherepy et al., 1994), they reported the Raman scattering with P resonance to be as much as 15 times *larger* than scattering from B. Cherepy et al. (1994) have discussed the possible reasons for these discrepancies. However, the fact that we observe very similar spectra from RCs obtained from different species (and different labs) provides support for the correctness of our results.

The comparison of the *C. aurantiacus* and *Rb. sphaeroides* spectra is useful in theoretically modeling the B spectrum. We used the Raman spectrum excited in the B band of *Rb. sphaeroides* as our model monomer Bchl spectrum, assuming that that B_A and B_B have the same Raman spectrum (Shreve et al., 1995). In *C. aurantiacus* only one Bchl monomer is present, so this spectrum must represent one Bchl monomer. Since the spectrum of B from *C. aurantiacus* is nearly identical to the *Rb. sphaeroides* B spectrum, this supports the assumption that the two Bchl monomers in the *Rb. sphaeroides* RC have similar Raman spectra. A Soret band excitation resonance Raman study of *Rb. sphaeroides* RCs also showed only very minor differences in modes in the high-frequency region between B_A and B_B (Beese et al., 1988). Since the relative intensities of the B modes in the *C. aurantiacus* and *Rb. sphaeroides* spectra do not differ, we can assign the two Bchl monomers, B_A and B_B, the same electron−nuclear coupling constants.

The similarity of the P and B spectra between *C. aurantiacus* and *Rb. sphaeroides* is consistent with a picture in which both RCs undergo the same type of nuclear and electronic dynamics upon excitation. The modes appearing in a resonance Raman spectrum correspond to the nuclear motions which couple the ground to the excited state. Thus, the similarity of these data demonstrates that the nuclear distortions that P and B undergo upon excitation are essentially the same in the two RCs. The absolute resonance Raman cross sections of P also do not change, suggesting that the electronic dephasing time for the excited state of P is the same in both RCs. Since both the absorption spectrum and resonance Raman cross sections are controlled by the same homogeneous linewidth and electron−nuclear coupling constants observed in the resonance Raman spectrum, the absolute intensities of the Raman modes can be analyzed in conjunction with the absorption spectrum to determine the excited-state dephasing time (Myers & Mathies, 1987). In fact, the weak Raman cross sections of P are most consistent

with a very rapid excited-state relaxation, on the order of tens of femtoseconds. This observation must be reconciled with the hole-burning experiments on the P band which have been fit to give an excited-state dephasing time of 1.2 ps at 1.5 K (Middendorf et al., 1993) and the oscillations observed in femtosecond emission studies from the excited state of P which decay with a *vibrational* dephasing time of about 1 ps (Vos et al., 1994). These observations may be understood, for instance, by a model in which multimode dephasing causes fast vibronic relaxation or by coupling of the optically prepared excited state to a dark state, such as a charge transfer band (Lathrop & Friesner, 1994). The observation of similar spectra and weak Raman cross sections from *C. aurantiacus* suggests that the excited-state structure and initial excited-state dynamics for P for both RCs proceed with very similar kinetics and nuclear distortions.[2]

In summary, the unique characteristics of the P and B spectra that we first observed in the *Rb. sphaeroides* resonance Raman data receive further confirmation with this independent set of measurements. These characteristics include the following: (1) enhanced low-frequency (30–200 cm^{-1}) modes in P and the lack of such strong activity in B, (2) no strong modes in the high-frequency region of the P or the B spectrum, and (3) very small absolute Raman cross sections with excitation in P. The fact that these traits are seen in both RCs suggests that these specifics of electronic and nuclear dynamics may be necessary to the functioning of the RC and of P as an electron donor.

ACKNOWLEDGMENT

The authors would like to thank A. P. Shreve for his assistance and helpful suggestions and S. G. Boxer for sparking our interest in this research area. We acknowledge Mr. M. Reus for isolating the reaction centers of *C. aurantiacus*.

REFERENCES

Allen, J. P., Feher, G., Yeates, T. O., Komiya, H., & Rees, D. C. (1987) *Proc. Natl. Acad. Sci. U.S.A. 84,* 5730–5734.

Becker, M., Nagarajan, V., Middendorf, D., Parson, W. W., Martin, J. E., & Blankenship, R. E. (1991) *Biochim. Biophys. Acta 1057,* 299–312.

Beese, D., Steiner, R., Scheer, H., Angerhofer, A., Robert, B., & Lutz, M. (1988) *Photochem. Photobiol. 47,* 293–304.

Boxer, S. G., Goldstein, R. A., Lockhart, D. J., Middendorf, T. R., & Takiff, L. (1989) *J. Phys. Chem. 93,* 8280–8294.

Cherepy, N. J., Shreve, A. P., Moore, L. J., Boxer, S. G., & Mathies, R. A. (1994) *J. Phys. Chem. 98,* 6023–6029.

Deisenhofer, J., Epp, O., Miki, K., Huber, R., & Michel, H. (1984) *J. Mol. Biol. 180,* 385–398.

Feher, G. (1989) *Annu. Rev. Biochem. 58,* 607–663.

Fleming, G. R., & van Grondelle, R. (1994) *Phys. Today 47,* 48–55.

Friesner, R. A., & Won, Y. (1989) *Biochim. Biophys. Acta 977,* 99–122.

Kirmaier, C., Blankenship, R. E., & Holten, D. (1986) *Biochim. Biophys. Acta 850,* 275–285.

Lathrop, E. J. P., & Friesner, R. A. (1994) *J. Phys. Chem. 98,* 3056–3066.

Mattioli, T. A., Hoffmann, A., Lutz, M., & Schrader, B. (1990) *C. R. Acad. Sci. Paris, Ser. III 310,* 441–446.

Middendorf, T. R., Mazzola, L. T., Lao, K., Steffen, M. A., & Boxer, S. G. (1993) *Biochim. Biophys. Acta 1143,* 223–243.

Müller, M. G., Griebenow, K., & Holzwarth, A. R. (1991) *Biochim. Biophys. Acta 1098,* 1–12.

Müller, M. G., Griebenow, K., & Holzwarth, A. R. (1992) *Chem. Phys. Lett. 199,* 465–469.

Myers, A. B., & Mathies, R. A. (1987) *Biological Applications of Raman Spectrometry: Vol. 2—Resonance Raman Spectra of Polyenes and Aromatics* (Spiro, T. G., Eds.) pp 1–58, John Wiley, New York.

Noguchi, T., Furukawa, Y., & Tasumi, M. (1991) *Spectrochim. Acta 47A,* 1431–1440.

Palaniappan, V., Aldema, M. A., Frank, H. A., & Bocian, D. F. (1992) *Biochemistry 31,* 11050–11058.

Palaniappan, V., Martin, P. C., Chynwat, V., Frank, H. A., & Bocian, D. F. (1993) *J. Am. Chem. Soc. 115,* 12035–12049.

Pierson, B. K., & Thornber, J. P. (1983) *Proc. Natl. Acad. Sci. U.S.A. 80,* 80–84.

Schweitzer, G., Hucke, M., Griebenow, K., Müller, M. G., & Holzwarth, A. R. (1992) *Chem. Phys. Lett. 190,* 149–154.

Shreve, A. P., Cherepy, N. J., Franzen, S., Boxer, S. G., & Mathies, R. A. (1991) *Proc. Natl. Acad. Sci. U.S.A. 88,* 11207–11211.

Shreve, A. P., Cherepy, N. J., & Mathies, R. A. (1992) *Appl. Spectrosc. 46,* 707–711.

Shreve, A. P., Cherepy, N. J., Moore, L. J., Franzen, S., Boxer, S. G., & Mathies, R. M. (1995) manuscript in preparation.

Shuvalov, V. A., Vasmel, H., Amesz, J., & Duysens, L. N. M. (1986) *Biochim. Biophys. Acta 851,* 361–368.

Volk, M., Scheidel, G., Ogrodnik, A., Feick, R., & Michel-Beyerle, M. E. (1991) *Biochim. Biophys. Acta 1058,* 217–224.

Vos, M. H., Jones, M. R., Hunter, C. N., Breton, J., Lambry, J.-C., & Martin, J.-L. (1994) *Biochemistry 33,* 6750–6757.

Woese, C. R. (1987) *Microbiol. Rev. 51,* 221–271.

Zankel, K., Reed, D., & Clayton, R. (1968) *Proc. Natl. Acad. Sci. U.S.A. 61,* 1243–1249.

BI9423704

[2] Because the overall electron–nuclear coupling in each frequency region of the *C. aurantiacus* and *Rb. sphaeroides* P spectra is very similar, the observed minor differences in the resonance Raman intensities and frequencies will produce insignificant changes in their vibronic models and in their calculated absorption spectra.